High Resolution Tip Enhanced Raman Mapping on Polymer Thin Films

L. Xue,[*1,2] *W. Li,*[1] *G. G. Hoffmann,*[1,2] *J. G. P. Goossens,*[1] *J. Loos,*[1,2,3] *G. de With*[1]

Summary: Advanced tip enhanced Raman mapping (TERM) was applied to high resolution chemical identification on nanoscale. Thin poly(methyl methacrylate)/poly(styrene acrylonitrile) (SAN28/PMMA) blend films were measured at different stages of phase separation. New insights into the phase evolution behavior of the thin films were obtained, when the TERM images were compared. An unexpected morphology transition was observed after a few minutes annealing at 250 °C. No surface enrichment of PMMA was observed, differing from the previous reports on a similar well-studied system of SAN33/PMMA. The glass transition temperature, the surface and interfacial tension were found to be the main factors responsible for the phase evolution behavior of SAN28/PMMA films.

Keywords: high resolution chemical identification; phase separation; polymer blend; thin film; tip enhanced Raman spectroscopy (TERS); tip enhanced Raman mapping (TERM)

Introduction

Thin polymer films are widely used for coatings, packaging materials, barriers, membranes, sensors and medical implants.[1,2] To achieve certain mechanical and functional properties, different polymers are blended with various additives. Good control over the morphology of the multi-component system and the miscibility of different components is essential to the ultimate properties.[3] To obtain insight into the phase separation behavior of the thin films, non-destructive characterizations of local morphology and chemical composition are equally important. For morphology studies, Atomic Force Microscopy (AFM) and Transmission Electron Microscopy (TEM) are often used. For chemical identification, deuteration and chemical etching are required when techniques like forward recoil spectrometry and AFM are used.[4–10] A prior knowledge of the sample chemical composition is required when destructive techniques are used. For non-destructive chemical analysis, confocal Raman spectroscopy was explored in this field. This method provides a better spatial resolution (~300 nm) compared to the micrometer scale resolution in Infra-Red (IR) and traditional Raman spectroscopy.[11–18] The recently developed non-destructive chemical identification techniques, tip enhanced Raman spectroscopy (TERS)/tip enhanced Raman mapping (TERM), provide a possibility for high resolution (~30 nm) chemical mapping.[19–25] The lateral resolution of TERM is independent on the incident laser wavelength due to the high local enhancement at the tip (about 30 nm at the end of the tip [20,26]). As a result, a short exposure time is sufficient for a high resolution TERM on a sample surface.[19,26,27] To ensure a constant enhancement factor during a relatively long TERM measurement, a sharp tip with stable mechanical and chemical properties is of great importance.

[1] Department of Chemical Engineering and Chemistry, Eindhoven University of Technology, P.O. Box 513, 5600 MB, Eindhoven, The Netherlands
E-mail: L.Xue@tue.nl
[2] Dutch Polymer Institute, P.O. Box 902, 5600 AX Eindhoven, The Netherlands
[3] Presently at the Department of Physics and Astronomy, University of Glasgow, Glasgow G12 8QQ, Scotland, United Kingdom

In this work, we present the enhancement of TERS in a polymer blend system, namely poly(methyl methacrylate)/poly-(styrene acrylonitrile) (SAN28/PMMA) thin films with a thickness of about 500 nm. Improved detection sensitivity is achieved due to the high enhancement factor. High resolution TERM images recorded on films at different stages of phase separation were compared. New insights were obtained into the phase evolution behavior of the SAN28/PMMA films. The new phase evolution behavior was analyzed based on the glass transition temperature, surface and interfacial tension. A comparison with a similar system of SAN33/PMMA was carried out to explain the differences observed in phase separation and wetting behaviors in our SAN28/PMMA case.

Experimental Part

Sample Preparation

Materials and the sample preparation method were described in details in another report.[26] The samples were spin-coated, dried at 150 °C for 5 h, annealed at 250 °C, and quenched to room temperature. The film thickness was typically ~500 nm. Early stage and intermediate stage phase separation were properly induced after 2 and 5 min. annealing to Film I and Film II, respectively.

Tip Preparation

A cone-shaped gold tip, with a typical radius of ~30 nm, was prepared by electrochemical etching as described in the literature.[20,27]

Measurement

Optical microscopy, TERS and TERM measurements were carried out using an NTEGRA SPECTRA™ (NT-MDT. Russia). A scanning near-field optical microscopy head (SNLG101NTF, NT-MDT, Russia) was placed above an inverted optical microscope (Olympus IX70). A self-etched gold tip, a 100× oil immersion objective (Olympus, NA = 1.3, refractive index $n = 1.516$), a pinhole of 40 μm and a continuous wave linearly polarized He-Ne laser (633 nm) were used for all measurements. A typical lateral/depth resolution about 20–30 nm is expected from the TERS/TERM measurements.[19]

Results and Discussion

Preparation for TERM Measurement

Optical images of PMMA/SAN blend films were first captured before any TERS/TERM measurements. Then a He-Ne laser was focused on the sample and the confocal Raman spectrum was recorded. The tip is then approached to the film surface. A reflection image of the cone-shaped gold tip was recorded by a tip scan. The tip is then aligned to the focus of the laser beam as described in a previous report.[20] The enhancement factor was calculated based on the ratio of the Raman intensity of certain characteristic Raman bands in TERS and confocal Raman spectra. The enhancement factor of TERS is dependent on the tip-sample distance, the smaller the distance, the better the enhancement. Therefore, the tip-sample distance was adjusted based on the maximum Raman intensity of certain characteristic Raman bands in the TERS spectrum.

The optical images of Film I were recorded when the tip was approached to and was withdrawn from the sample surface as shown in Figure 1(a) and (b), respectively. The bright area in both images appeared to have the same pattern, indicating the reflection of the optical light from the tip (cone-shaped in black). We noticed this reflection pattern was moving in position during landing, but retaining its shape. This reflection pattern was found helpful during the alignment of the tip. It was more difficult to find the image of the tip (of a few micrometer) than to find its reflection patten (of hundred's of micrometer). When the tip was approached, the image of the tip became sharp as shown in Figure 1(a).

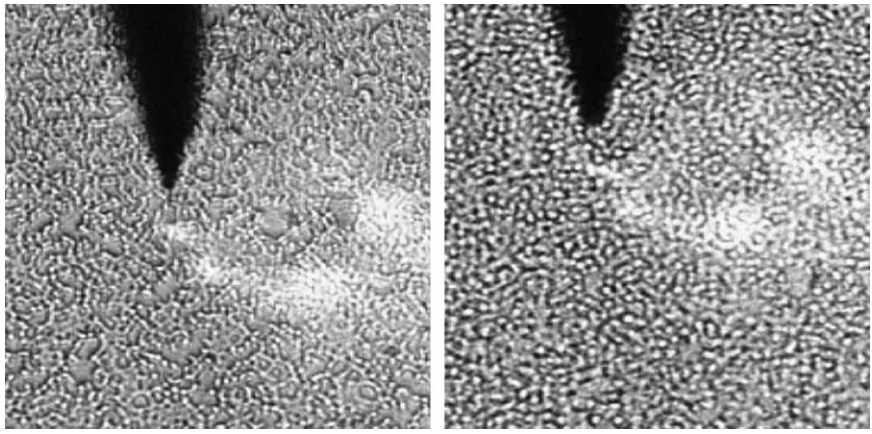

Figure 1.
Optical images captured when a cone-shaped gold tip is (a) landed on and (b) withdrawn from the surface of Film I. A 100× oil immersion objective (Olympus, NA = 1.3, refractive index of the oil $n = 1.516$) was used.

High Resolution TERM

High enhancement of TERS signals for polymers was recently reported as shown in Figure 2.[26] There was a 15 times linear enhancement in terms of the maximum Raman intensity. The enhancement factor was greater than 1500 taking the 100 times smaller probing area into account. In ref.,[26] the TERM images based on the maximum Raman intensity of different characteristic Raman bands for PMMA and SAN were compared. PMMA-rich and SAN-rich phases were found to be corresponding to the bright and the grey phases in Figure 1, respectively. An interface width of about 200 nm was observed at the boundary region between the two phases.

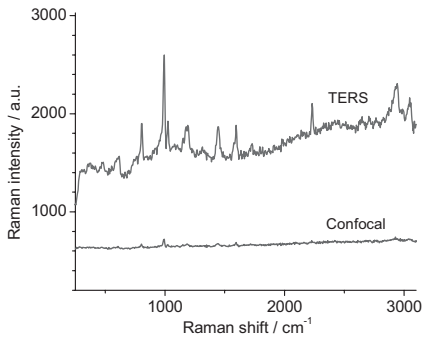

Figure 2.
The high enhancement of TERS (upper line), as compared to the confocal Raman spectroscopy (lower line).

In this work, the chemical distribution was directly visualized based on the shifts of the mass center and the peak position of the Raman band at $\sim 1000\,cm^{-1}$. The TERM measurements were performed over an area of $10\,\mu m \times 10\,\mu m$ with a nominal pixel size of 40 nm and an exposure time of 5 s/point. The Raman band at $\sim 1000\,cm^{-1}$ from SAN was found to be at a higher Raman shift than that of PMMA, as indicated in Figure 2 from ref. [26]. The distribution of SAN was found to form a continuous pattern, green in Figure 3(a) and red in Figure 3(b), respectively. Therefore the counter phase was suggested to be PMMA-rich, in agreement with what has been reported before.[26]

In this paper we would like to show the improved detection sensitivity due to the high enhancement factor of TERS. Since the volume probed by TERM on each point of the sample is about > 3000 smaller than that of the traditional confocal Raman,[26] it is possible to detect the chemical nature of phase domains as small as ten's of nanometer. We found that small (green and red) clusters of SAN were clearly observed in the (blue and green) domains of PMMA in Figure 3(a) and (b), and vice versa. The same phenomena were

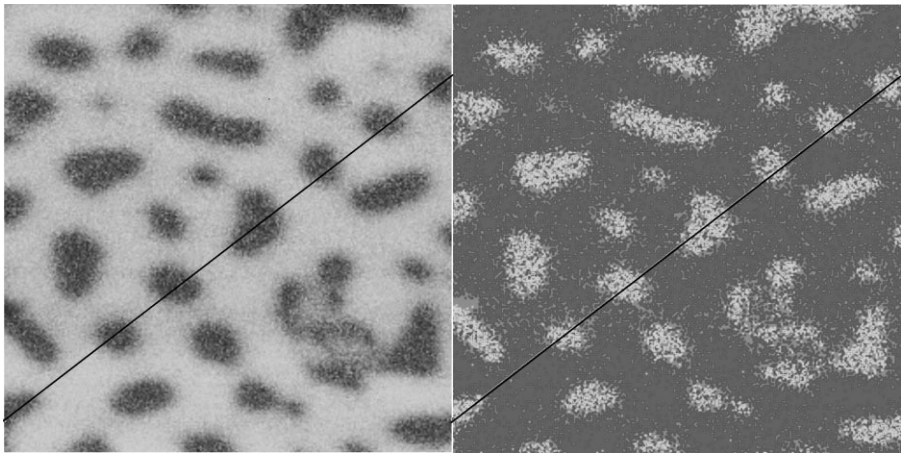

Figure 3.
TERM images of Film I, 10 μm x 10 μm, based on the Raman shift of (a) the mass center and (b) the peak position of Raman band at $\sim$ 1000 cm^{-1}. Raman shift profiles in Figure 3 were taken along the black lines.

only observed in the zoom-in (1 μm × 1 μm) TERM results in terms of the maximum Raman intensity.[26]

Shift profiles of the Raman band's mass center position as well as its maximum intensity position were then compared across the sample. As shown in Figure 4, The Raman shift profiles were taken along the lines in Figure 3. The traces in green and red represent the Raman shifts of the mass center position and the maximum intensity position of the Raman bands at $\sim$1000 cm^{-1}. The Raman bands from PMMA and SAN are very different in this region, being very weak and broad for PMMA, and very strong and very sharp for SAN, as shown in a previous report [26] in Fig. 2. The presence of a small amount of SAN may lead to a big shift of the maximum intensity position, while the shift of the mass center position may be undetectable. The Raman shift of the mass center position, green in Figure 4, appears to change along the sample surface in a much smoother manner while that of the maximum intensity position was jumpy. The mass center position of two partially overlapping Raman bands varies with composition changes, as indicated in the slopes of the green curve. Compared to the reported concentration gradients from one to another phase in the previous report,[26] the Raman shift curve of the mass center position appears to have the same trend as the concentration gradient.

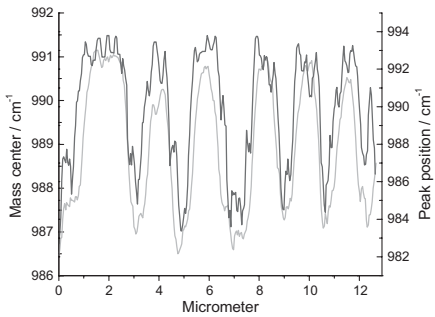

Figure 4.
Shift profiles of (a) the mass center position (lower curve) and (b) the maximum intensity position (upper curve) of the characteristic Raman bands at $\sim$ 1000 cm^{-1}. The profiles were taken along the lines (in black) indicated in Figure 3.

The reported boundary concentration gradient from one phase to another was not directly visible from the TERM images in Figure 3. The concentration gradient can be better observed from a 3D TERM image in terms of the Raman shift of the mass center of the corresponding Raman bands at $\sim$1000 cm^{-1} in Figure 5.

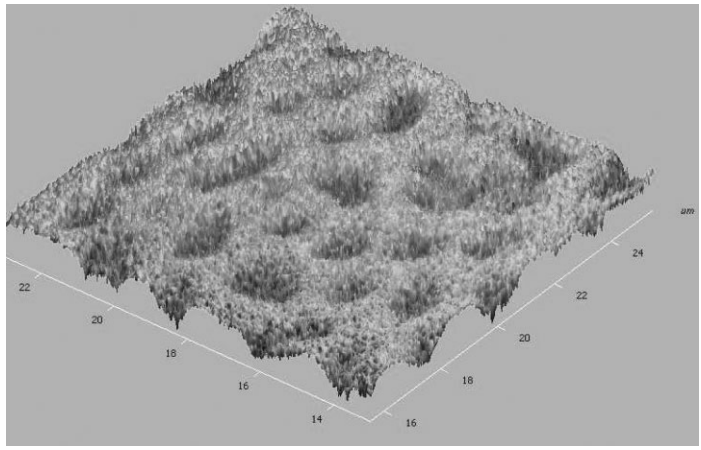

Figure 5.
3D representation of TERM image shown in Figure 2 (a).

On the other hand, the curve of the peak position follows the same trends as shown in Figure 4 (the trace in red), not only crossing the boundary region but also appearing in the other phase. This again indicates a high detection sensitivity of TERM, in this case from the mapping of the peak position of a certain Raman band.

New Insights into the Phase Separation Behavior

A wetting layer of the low surface energy component PMMA was observed in a similar system.[12] If there were such enrichment of PMMA in the current SAN28/PMMA case, we should have observed strongly-enhanced PMMA Raman bands, since the nearer the sample to the tip, the stronger the enhancement should be.[20] Surprisingly, no obvious PMMA Raman bands were observed from the TERS and confocal Raman spectra as reported in the previous paper.[26] AFM height images of both Film I and Film II are presented in Figure 6. The maximum height differences are $<10\,\text{nm}$ and $\sim 70\,\text{nm}$ for Film I and Film II, respectively. No spherical collapsing of the cap on the little hills shown in Film I, indicating a PMMA wetting layer, was observed in Figure 6(a). This was found to be due to the differences between the two systems, as listed in Table 1.

The 3D TERM images of both films are shown in Figure 7, in terms of the maximum Raman intensity of the characteristic Raman band at $\sim 1002\,\text{cm}^{-1}$ for SAN, respectively. The interconnected little hills shown in Figure 6 (a) were found to be the continuous SAN-rich phase in Figure 7 (a). The dark brown counter phase is PMMA-rich.

Using certain TERM measurement settings, the tip was moving along the sample surface by keeping the same tip–sample distance. Hence the enhancement factor was constant. Therefore we can estimate the concentration of a certain component based on the maximum Raman intensity. The slope of the hills indicates a continuous concentration gradient of SAN species at the boundary interface region. Therefore, it again suggests that the early stage phase separation produced PMMA-rich phase domains discretely dispersed in the continuous SAN-rich phase. The SAN-rich domains were found to grow in size and the concentration of the SAN-rich phase appeared to reach a constant value, as shown in Figure 7 (b). This also suggests that Film II was at the intermediate stage of phase separation. The unexpected mor-

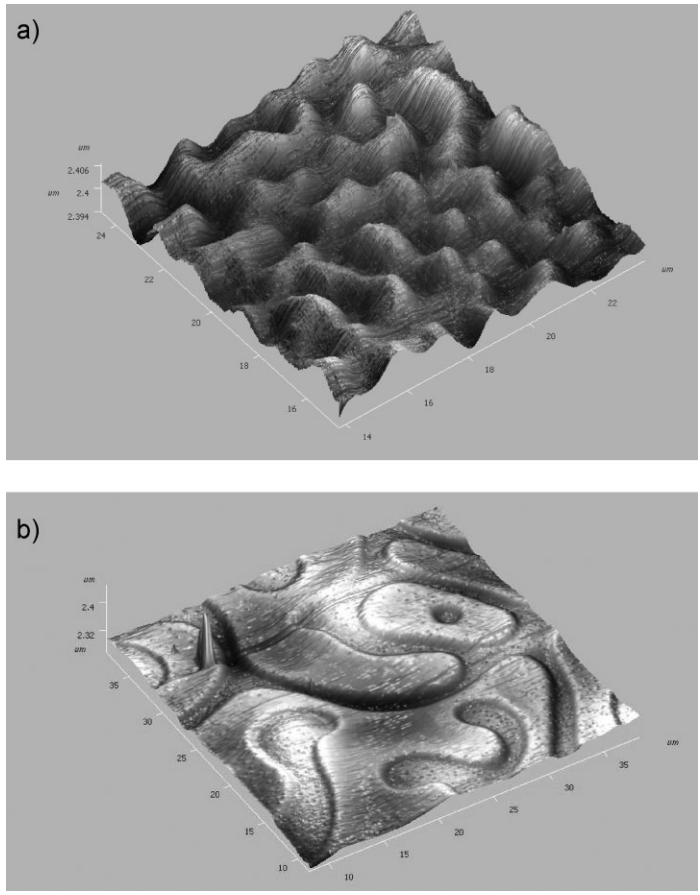

Figure 6.
AFM height images of (a) Film I and (b) Film II, using non-contact mode.

phology transition in the SAN28/PMMA system, reported in ref.,[26] might also be partly due to the much smaller interfacial tension as compared to the SAN33/PMMA system.

The phase evolution kinetics of the current system was found to be different from that of the SAN33/PMMA.[12] In the current SAN 28/PMMA system the SAN has a lower T_g (~115 °C), so that phase separation is likely to proceed via the formation of a SAN-rich continuous phase. Because the interfacial energy of the SAN/PMMA is only 0.15 mJ/m^2, this process is

Table 1.
Comparison between the SAN33/PMMA [26] and the SAN28/PMMA systems.[26]

	SAN28/PMMA	SAN33/PMMA
Composition	SAN28, (28% AN)	SAN33, (33% AN)
Glass transition temp.	T_g (PMMA) ~120 °C	T_g (PMMA) ~105 °C
Substrate	glass, rough	silicon, flat
Duration of the phase separation	fast phase separation (in minutes)	slow phase separation (in hours)
Interfacial energy	0.15 mJ/m^2	1 mJ/m^2

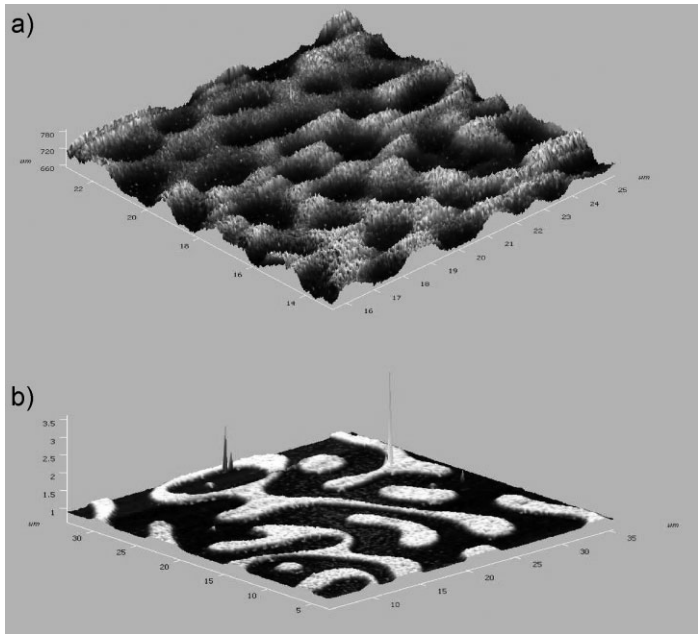

Figure 7.
The 3D TERM images of (a) Film I and (b) Film II in terms of the maximum Raman intensity of the characteristic Raman bands at $\sim 1002\,cm^{-1}$ for SAN.

not too much hampered and the structure is kinetically determined in Film I. The early stage phase separation behavior in SAN28/PMMA was found to be induced by the higher mobility of the SAN chains, due to its 5 °C higher glass transition temperature and the 10% higher surface energy than PMMA. After longer annealing time, thermodynamics takes over so that a morphology change occurs, yielding morphology of Film II similar as reported in ref. [12]. We speculate that in the SAN33/PMMA system [12] having a large interfacial energy and a small T_g of the low surface energy component, a bi-continuous morphology (Film II) should appear directly or much faster.

Conclusion

Using a cone-shaped gold tip, up to 15 times linear enhancement was achieved using TERS, compared to conventional confocal Raman spectroscopy. The enhancement factor was greater than 1500 when taking the 100 times smaller probing area into account.

Due to the enhancement effect, the detection sensitivity of TERS/TERM was improved for macromolecular systems. This allowed a detailed chemical analysis on the nanoscale. In the interfacial/interphase region, the interface width and the concentration gradient were directly visualized.

To summarize, the TERS/TERM technique can be very promising for trace-amount chemical analysis/identification of macromolecular systems.

Acknowledgements: We are grateful for the financial support by Dutch Polymer Institute (DPI) (grant #692) and technical support by NT-MDT.

[1] H. Wang, R. J. Composto, *Macromolecules* **2002**, *35*, 2799–2809.

[2] Y. Liao, Z. Su, X. Ye, Y. Li, J. You, T. Shi, L. An, *Macromolecules* **2005**, *38*, 211–215.
[3] M. Stamm, D. W. Schubert, *Annu. Rev. Mater. Sci.* **1995**, *25*, 325–356.
[4] H. J. Chung, A. Taubert, R. D. Deshmukh, R. J. Composto, *Europhysics Letters* **2004**, *68*, 219–225.
[5] H. J. Chung, R. J. Composto, *Physical Review Letters* **2004**, *92*, 185704.
[6] H. Wang, R. J. Composto, *Journal of Chemical Physics* **2000**, *113*, 10386–10397.
[7] H. Wang, R. J. Composto, *Physical Review E* **2000**, *61*, 1659–1663.
[8] B. Z. Newby, R. J. Composto, *Macromolecules* **2000**, *33*, 3274–3282.
[9] H. Wang, R. J. Composto, *Europhysics Letters* **2000**, *50*, 622–627.
[10] H. J. Chung, H. Wang, R. J. Composto, *Macromolecules* **2006**, *39*, 153–161.
[11] S. Huan, W. Lin, H. Sato, H. Yang, J. Jiang, Y. Ozaki, H. Wu, G. Shen, R. Yu, *J. Raman Spectroscopy* **2007**, *38*, 260–270.
[12] U. Schmidt, S. Hild, W. Ibach, O. Hollricher, *Macromol. Symp.* **2005**, *230*, 133–143.
[13] P. Schmidt, J. Dybal, J. Šťudla, M. Raab, J. Kratochvil, *Macromol. Symp.* **2002**, *184*, 107–122.
[14] A. M. MacDonald, A. S. Vaughan, P. Wyeth, *Applied Spectroscopy* **2003**, *57*, 1475–1481.
[15] J. C. Merino, M. del R. Fernández, J. M. Pastor, *Macromol. Symp.* **2001**, *168*, 55–65.
[16] P. Schmidt, J. Kolařík, F. Lednický, J. Dybal, J. M. Lagarón, J. M. Pastor, *Polymer* **2000**, *41*, 4267–4279.
[17] L. Quintanilla, J. C. Rodríguez-Cabello, T. Jawhari, J. M. Pastor, *Polymer* **1994**, *35*, 514–518.
[18] P. Schmidt, M. R. Fernandez, J. M. Pastor, J. Roda, *Polymer* **1997**, *38*, 2067–2075.
[19] B.-S. Yeo, E. Amstad, T. Schmid, J. Stadler, R. Zenobi, *Small* **2009**, *5*, 952–960.
[20] S. S. Kharintsev, G. G. Hoffmann, P. S. Dorozhkin, G. de With, J. Loos, *Nanotechnology* **2007**, *18*, 315502.
[21] L. Novotny, S. J. Stranick, *Annu. Rev. Phys. Chem.* **2006**, *57*, 303–331.
[22] B. Pettinger, B. Ren, G. Picardi, R. Schuster, G. Ertl, *J. Raman Spectroscopy* **2005**, *36*, 541–550.
[23] D. Richards, R. G. Milner, F. Huang, F. Festy, *J. Raman Spectroscopy* **2003**, *34*, 663–667.
[24] R. M. Stöckle, Y. D. Suh, V. Deckert, R. Zenobi, *Chemical Physics Letters* **2000**, *318*, 131–136.
[25] A. Hartschuh, M. R. Beversluis, A. Bouhelier, L. Novotny, *Phil. Trans. R. Soc. Lond. A* **2004**, *362*, 807–819.
[26] L. Xue, W. Li, G. G. Hoffmann, J. G. P. Goossens, J. Loos, G. de With, *Macromolecules* **2011**, in press
[27] B. Ren, G. Picardi, B. Pettinger, *Rev. Sci. Instrum.* **2004**, *75*, 837.

